General Disclaimer

One or more of the Following Statements may affect this Document

- This document has been reproduced from the best copy furnished by the organizational source. It is being released in the interest of making available as much information as possible.

- This document may contain data, which exceeds the sheet parameters. It was furnished in this condition by the organizational source and is the best copy available.

- This document may contain tone-on-tone or color graphs, charts and/or pictures, which have been reproduced in black and white.

- This document is paginated as submitted by the original source.

- Portions of this document are not fully legible due to the historical nature of some of the material. However, it is the best reproduction available from the original submission.

Produced by the NASA Center for Aerospace Information (CASI)

SQT

(NASA-CR-162358) CHARGE-EXCHANGE PLASMA ENVIRONMENT FOR AN ION DRIVE SPACECRAFT (Jet Propulsion Lab.) 37 p HC A03/MF A01 CSCL 21C

N79-33251

Unclas G3/20 38895

Charge-Exchange Plasma Environment for an Ion Drive Spacecraft

Harold R. Kaufman
Colorado State University
M. Ralph Carruth, Jr.
Jet Propulsion Laboratory

October 1, 1979

National Aeronautics and
Space Administration

Jet Propulsion Laboratory
California Institute of Technology
Pasadena, California

JPL PUBLICATION 79-90

Charge-Exchange Plasma Environment for an Ion Drive Spacecraft

Harold R. Kaufman
Colorado State University
M. Ralph Carruth, Jr.
Jet Propulsion Laboratory

October 1, 1979

National Aeronautics and
Space Administration

Jet Propulsion Laboratory
California Institute of Technology
Pasadena, California

ABSTRACT

It is necessary to have an understanding of the charge-exchange plasma environment around a spacecraft that uses mercury ion thrusters for propulsion so that the interactions between this environment and the spacecraft can be determined. A model is reviewed which describes the propagation of the mercury charge-exchange plasma and extended to describe the flow of the molybdenum component of the charge-exchange plasma. The uncertainties in the models for various conditions are discussed throughout this report. Such topics as current drain to the solar array, charge-exchange plasma material deposition, and the effects of space plasma on the charge-exchange plasma propagation are addressed.

PRECEDING PAGE BLANK NOT FILMED

CONTENTS

PRECEDING PAGE BLANK NOT FILMED

CONTENTS (cont)

Figure

A. INTRODUCTION

Ion thrusters will be used in the near future as a primary propulsion device for interplanetary spacecraft and for attitude control and orbit transfer of spacecraft near earth. Because of the plasma environment produced by the thruster it is important to understand how this propulsion device will affect various spacecraft subsystems. An interplanetary spacecraft will likely be most affected by the ion thruster environment because of the use of multiple thrusters and thrusting periods of years.

This paper will describe the charge-exchange plasma environment produced by the thrust subsystem and how this environment will interact with the spacecraft. The effect that the space plasma will have on the charge-exchange plasma will also be addressed.

In order to describe the thruster produced environment, the various ion species emitted by a thruster are described. To distinguish the various ion species emitted by an ion thruster the notation of group I, group II, group III, and group IV ions was introduced.[1] The group I ions are those of the primary beam which travel downstream within a cone that has a small divergence. They are accelerated by the total potential difference between the bombardment discharge and the neutralized thrust beam. Group II ions are energetic ions that leave a thruster at angles up to nearly 90 degrees to the beam axis.[1] They are formed by charge-exchange between the screen and accelerator grids of the thruster optics. The group III ions are charge-exchange ions that are formed just downstream of the accelerator grid. These ions are drawn back into the acceleration grid by its negative potential. This produces a sputtered efflux from the accelerator optics that is somewhat more peaked (in the downstream direction) than a cosine distribution.[2-5] The neutrals which leave the thruster do so in approximately a cosine distribution.[6] All of the preceding effluxes are essentially limited to line-of-sight trajectories from the ion optics of the thruster.

Two other efflux categories, the group IV ions, are not limited to line-of-sight trajectories, and therefore can pose special spacecraft contamination problems. These effluxes are the low-energy mercury and molybdenum charge-exchange ions that are generated downstream of a thruster.[6,7] Because these effluxes are low energy ions, the trajectories can depart substantially from straight lines due to only moderate electric fields. The natural tendency is

for less dense regions of the charge-exchange plasma to be negative relative to the dense regions, so that ion trajectories are bent from the more dense to the less dense regions. As a result, the entire volume around a spacecraft becomes filled with charge-exchange plasma, with the density of this plasma depending on the ease of access from the region of generation downstream of a thruster. The charge-exchange plasma is macroscopically neutral so that everywhere electron density equals ion density.

The propagation of a charge-exchange plasma from a thruster has been the subject of study[8-10] due to the possible interactions with spacecraft. Further study of this propagation is expected. This report is intended as a summary of the present understanding of this propagation, interaction effects thereof, and possible verification experiments. The limitations of this present understanding will also be given, where possible. The calculations presented in this report will be limited to mercury propellant and molybdenum grid material, although the process with other materials would be expected to differ mostly due to different cross sections and yield coefficients. All equations presented herein are in SI (mks) units unless otherwise stated.

B. MERCURY CHARGE-EXCHANGE MODEL

The Hg charge-exchange model presented here is essentially the same as one presented in a previous publication.[10] The assumed point of origin for the Hg charge-exchange plasma is indicated in Fig. 1. For a single thruster, this point is one thruster radius, r_t, downstream of the ion optics and on the thruster centerline, as indicated in Fig. 1(a). This point was selected because it gave the best correlation of experimental data from several tests.

For a circular array of thrusters, the effective point of origin would be expected to be one radius of the thruster array, r_t' (see Fig. 1(b)), downstream of the center of the array. For a noncircular array, the effective origin would be expected to be downstream of the center of the array, between half the maximum array dimension and half the minimum array dimension. A noncircular array would also be expected to cause some departures from axial symmetry in the distribution of Hg charge-exchange plasma. But, because Hg charge-exchange measurements have not been made with thruster arrays, the exact extent of these departures from axial symmetry is not known.

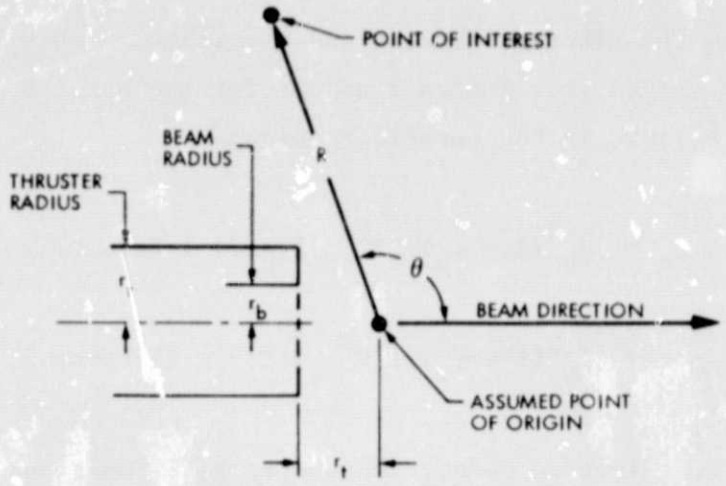

(a) SINGLE THRUSTER

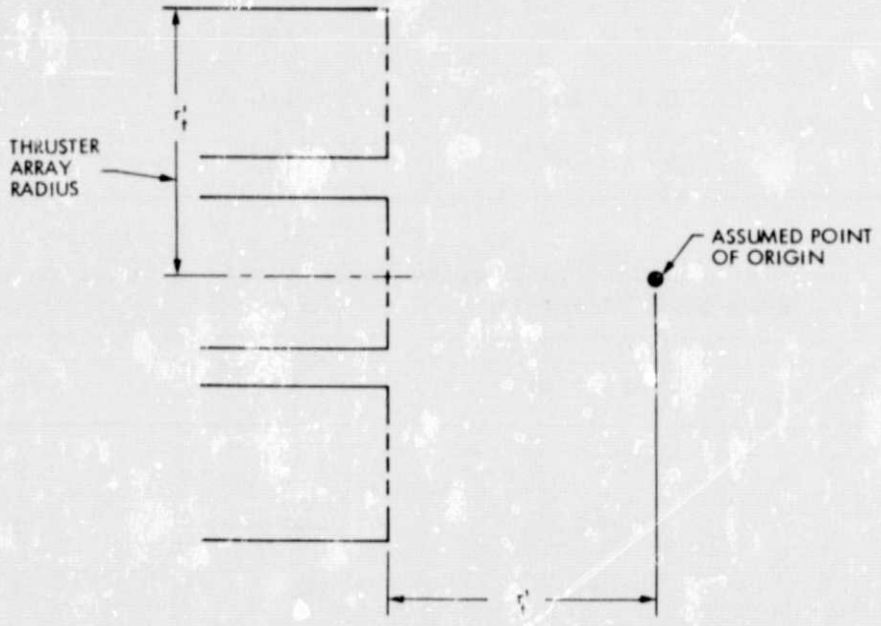

(b) THRUSTER ARRAY

Figure 1. Parameters for Calculation of Charge-Exchange Plasma Generated by Thruster.

To calculate the electron density and saturation electron current density, select parameter values from Tables I and II for the angle θ (see Fig. 1) of interest and substitute in the equations below:

$$n_e = [J_b^2(1 - \eta_u)/r_b R^2 \eta_u][\text{Table I Param.}],\ m^{-3} \quad (1)$$

$$j_e = [J_b^2(1 - \eta_u)/r_b R^2 \eta_u][\text{Table II Param.}],\ Am^{-2} \quad (2)$$

Table I. Electron Density Parameter as a Function of Angle from a Beam Direction

θ, Deg.	Parameter	θ, Deg.	Parameter
90	2.5×10^{12}	140	3.2×10^{11}
100	1.8×10^{12}	150	1.9×10^{11}
110	1.2×10^{12}	160	1.1×10^{11}
120	8.2×10^{12}	170	6.7×10^{10}
130	5.1×10^{11}	180	3.8×10^{10}

Table II. Electron Current Density Parameter as a Function of Angle From Beam Direction

θ, Deg.	Parameter	θ, Deg.	Parameter
90	0.12	140	0.017
100	0.091	150	0.011
110	0.064	160	0.0059
120	0.044	170	0.0034
130	0.028	180	0.0022

The beam current, J_b, is in amperes (A). It is the total current such that if a beam is produced by six thrusters each operating at 2A, J_b will be 12A. The propellant utilization, η_u, is a dimensionless quantity which can be expected to

$\mu \approx -0.9$. The beam radius, r_b, and the radius R are defined by Fig. 1. Both are measured in meters.

Tables I and II represent the mean values of experimental data. The upstream hemisphere (90-180 deg. from beam direction) is the region of most interest. In this hemisphere the data ranged upwards and downwards from the values used for Tables I and II by about a factor of two.

For electron density, the electron temperature is also a consideration. The production rate of charge-exchange ions is independent of electron temperature, but the velocity of departure for these ions varies as the square-root of electron temperature. To the first approximation, then, ion (and electron) density will vary inversely as the square-root of electron temperature. From available data, the electron temperature in the charge-exchange plasma around the thruster is about half of the electron temperature in the ion beam. The data used for Tables I and II had electron temperatures in the charge-exchange plasma of 2.5 and 3.5 eV. These values are believed representative of 5-15 cm Hg ion thrusters. The electron temperature within a 30-cm Hg thruster beam was found to be 0.35 eV.[11] Including the factor of two lower electron temperature in the charge-exchange plasma, a 30-cm thruster would be expected to have about a factor of four higher electron density than given by Eq. (1) with the parameter values listed in Table I.

The scaling of electron density inversely as the square-root of electron temperature, as described above, is actually of limited accuracy. Another consideration is the directed neutral velocity before charge exchange. Because the neutral temperature varies only slightly between different sizes of thrusters, this initial velocity is much more significant where electron temperatures are small. We do not know the magnitude of this effect, but we do know its direction. The initial downstream neutral velocity of charge-exchange ions will bias their distribution towards the downstream direction, thus reducing their density in the upstream hemisphere. Because of the smaller plasma electron energy in large thrusters, this effect will be most noticeable in such thrusters. The additional effect of neutral velocity, beyond the density varying inversely as the square-root of electron temperature, should make the actual electron density lower than the calculated values for 30-cm thrusters in the upstream hemisphere. At present, the magnitude of the reduction is not known.

Electron temperature is not as important for the saturation electron current density. Except for the bias due to initial neutral velocity, the effects of electron temperature cancel for electron current density.

The ion arrival rate is closely related to the saturation electron current. The ion velocity can be closely approximated by the Bohm, or ion acoustic, velocity based on electron temperature in the ion beam.[8,9] The electron velocity is, of course, a Maxwellian distribution corresponding to the temperature in the charge-exchange plasma. For a surface normal to the local ion velocity, the ratio of ion current to electron saturation current is

$$j_i/j_e = 2\sqrt{\pi m_e/m_i} = 5.9 \times 10^{-3}. \tag{3}$$

It should be kept in mind that the ion velocity is substantially directed, while that of the electrons is isotropic. With this limitation in mind, Eq. (3) can be used to obtain ion current densities from Eq. (2). For convenience the following extension to Eq. (3) gives the time (t) in seconds for a monolayer to form. This is assuming that the surface is cold enough to condense all the mercury arriving there. Also, the theory does not allow for geometrical considerations such as shielding. Shielding may act to reduce the arrival rate but the charge-exchange plasma will be able to flow around obstructions.

$$t = 3.3 \times 10^2/j_e \tag{3a}$$

1. Sample Calculation for Spacecraft

A sample calculation, using the charge-exchange plasma model described, is performed to illustrate the variation in plasma and current densities around a typical spacecraft. The spacecraft has an assumed configuration which utilizes eight 30-cm thrusters[12] arranged in two parallel rows of four each. Each row of four has center-to-center spacings of 76 cm, while the center-to-center spacing between the two rows of four is 51 cm. The two solar array panels extend radially outwards from the axis of the spacecraft, with the inside end of the panels starting 254 cm from the spacecraft centerline and 432 cm upstream of the thruster exhaust plane.

The calculation procedure used is that described above. Seven of the eight thrusters are assumed to be operating at a beam current of 2A each with a propellant utilization of 0.9. The other thruster is not operating. Although the nominal diameter is 30 cm for these thrusters, the actual beam diameter is closer to 28 cm.

The charge-exchange plasma is assumed to have an electron temperature equal to half the measured ion-beam electron temperature (from single thruster tests) of 0.35 eV. This lower electron temperature, compared to the data used for Tables I and II, should result in an electron density increase of about $20^{\frac{1}{2}}$. As mentioned above, there is no similar correction for the current density parameter. Another assumption concerns the point of origin for the charge-exchange plasma.

For the non-circular thruster array of this spacecraft, the total array area is equivalent to a circle with a radius of 0.885 m. The effective origin of the charge-exchange plasma is assumed to be 0.885 m downstream of the center of the thruster array. Some nonsymmetry of the charge-exchange plasma about the thrust axis is expected to result from the nonsymmetrical distribution of thrusters, but the charge-exchange plasma will tend to redistribute itself so as to reduce this effect. The maximum increase in electron density or electron current is therefore estimated at less than a factor of two for a distance of one meter or more from the thruster array. (This factor increases the overall uncertainty to about a factor of four.)

The plasma properties at the centerline of the solar array were calculated as a function of distance from the inboard end of the solar array and plotted in Fig. 2. The combined effects of radial distance, R, and angle, θ, give maximum electron density and current density near, but not at, the inboard end of each solar array. For the assumed dimensions of 3.8 m x 44.3 m for each array, the integrated total of the current density shown in Fig. 3 is 1.7 A for both arrays. This current includes no increase in effective array size due to sheath thickness. The electron density ranges from about 1 to 12 x 10^{11} m^{-3}, which, at 0.175 eV, corresponds to a range from 3 mm to 1 cm in Debye distance. For a solar array that is 400 V positive of the surrounding plasma, for example, the total sheath thickness would range from about 20 to 60 cm. The effect of sheath thickness can clearly be significant, but will not change the qualitative effects shown in Fig. 3.

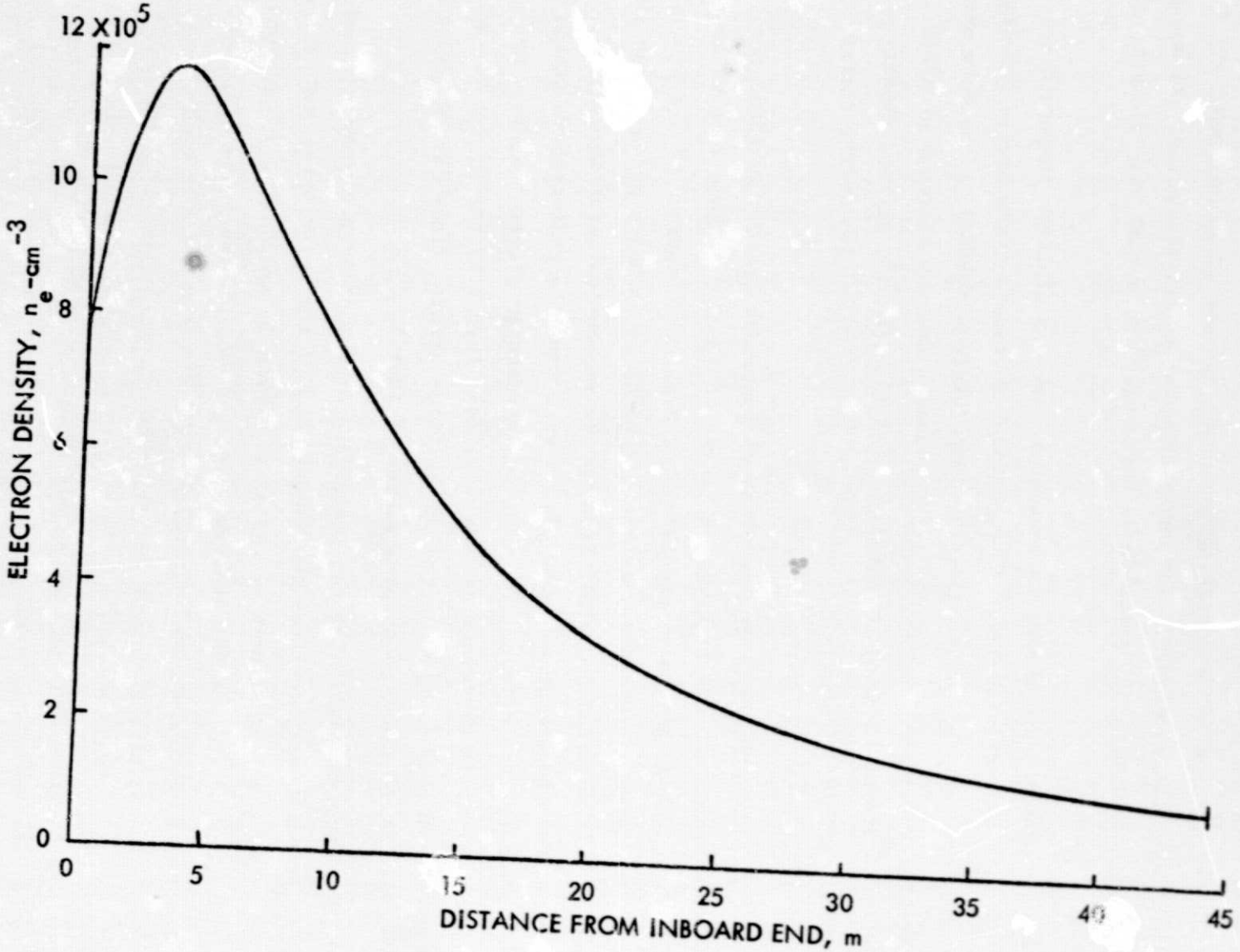

Figure 2. Electron Density Along Centerline of Solar Array

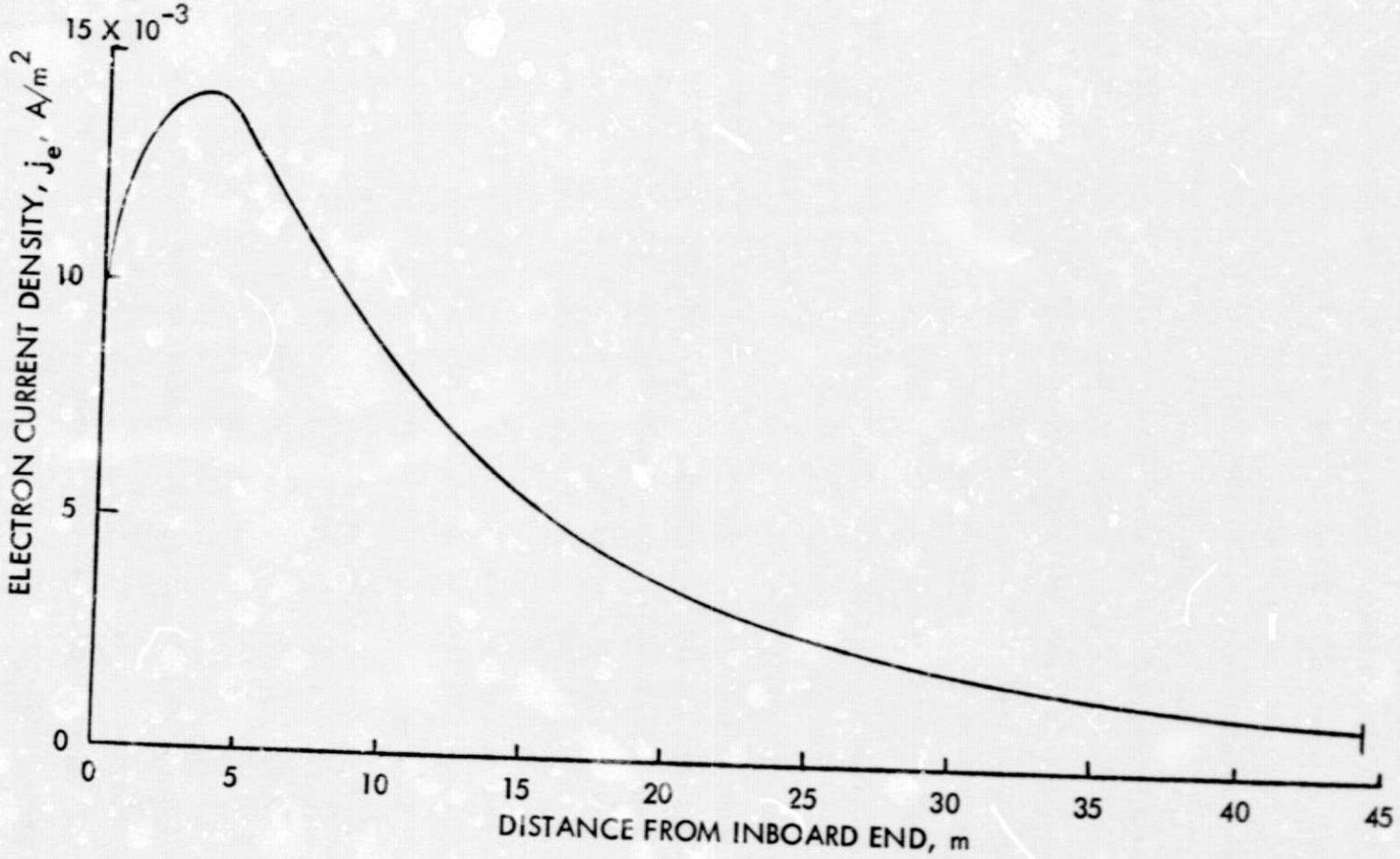

Figure 3. Saturation Electron Current Density Along Centerline of Solar Array

The locations on the spacecraft correspond to wide ranges of both radial distance, R, and angle from beam direction, θ. Two dimensional plots of electron density and saturation electron current density are shown in Figs. 4 and 5. Both plan and side views of the assumed spacecraft are shown in each of these figures. The assumed point of origin for the charge-exchange plasma is indicated in Figs. 4 and 5 and is, as was mentioned previously, 0.885 m downstream of the center of the thruster-array exhaust plane. As shown in Fig. 4, the expected electron density can range from about 10^5 to 10^7 cm^{-3}. In Fig. 5, the saturation electron current density is shown to range from 1 to 100 mA/m^2. From Fig. 5 and Eq. (3) the corresponding arrival rate of Hg ions would range from 6 to 600 $\mu A/m^2$. Figure 6 shows the arrival rate of Hg in terms of monolayer formation. One monolayer of mercury is $\sim$2.9Å.

As mentioned, seven operating thrusters were assumed for the calculations whose results are shown in Figs. 2 through 6. For fewer thrusters or less than rated operating conditions, both the electron densities and the electron and ion current densities would have to be reduced. For fewer operating thrusters, these parameters should be reduced in proportion to the number of thrusters. For less than rated conditions, the plasma parameters would be proportional to $J_b^2(1 - \eta_u)/\eta_u$. For the usual throttled operation near the discharge-performance "knee", $J_b^2(1 - \eta_u)/\eta_u$ will be nearly proportional to J_b.

The orientation of a surface relative to the propagation of the charge-exchange plasma will influence the density and arrival rates observed at the surface. Some reduction of these parameters would be expected for more protected surface orientations and surfaces that are locally shielded by parts of the spacecraft. Because of the proven capability of a charge-exchange plasma to flow around corners, the amount of this reduction cannot be estimated at the present time.

A variety of devices has been suggested and tried for diverting or collecting the charge-exchange plasma. Shields near the thruster can displace or divert the charge exchange plasma, but do not appear to significantly reduce the number of charge-exchange ions that escape to the surrounding volume,[9] presumably because electric fields do not extend far into the plasma. Positive surfaces will repel charge-exchange ions, but the large electron currents also collected will usually make this approach impractical. Insulated surfaces will draw equal numbers of electrons and ions, which means that all of the arriving ions will be collected

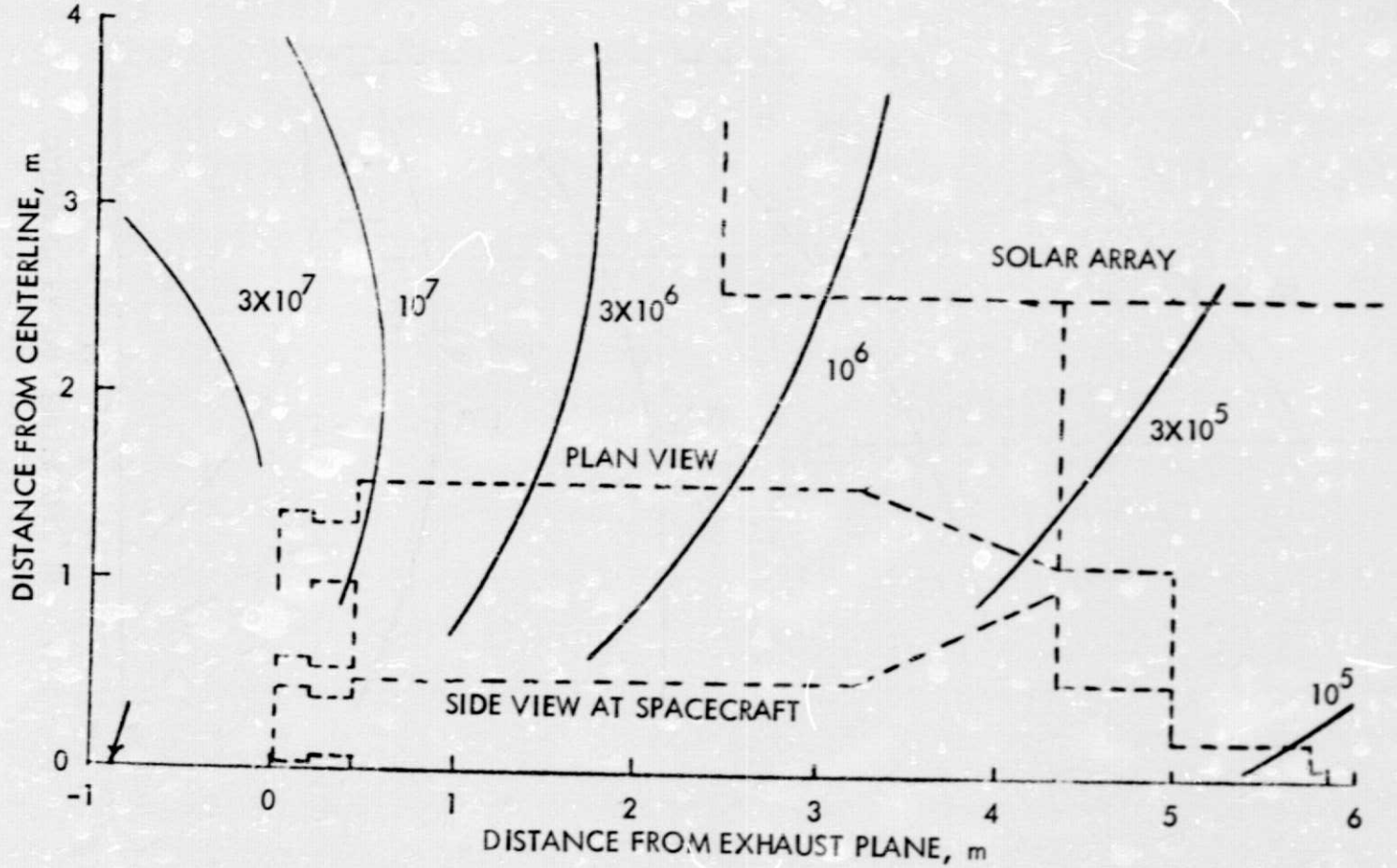

Figure 4. Electron Density, n_e, cm^{-3}, for Assumed Spacecraft Configuration

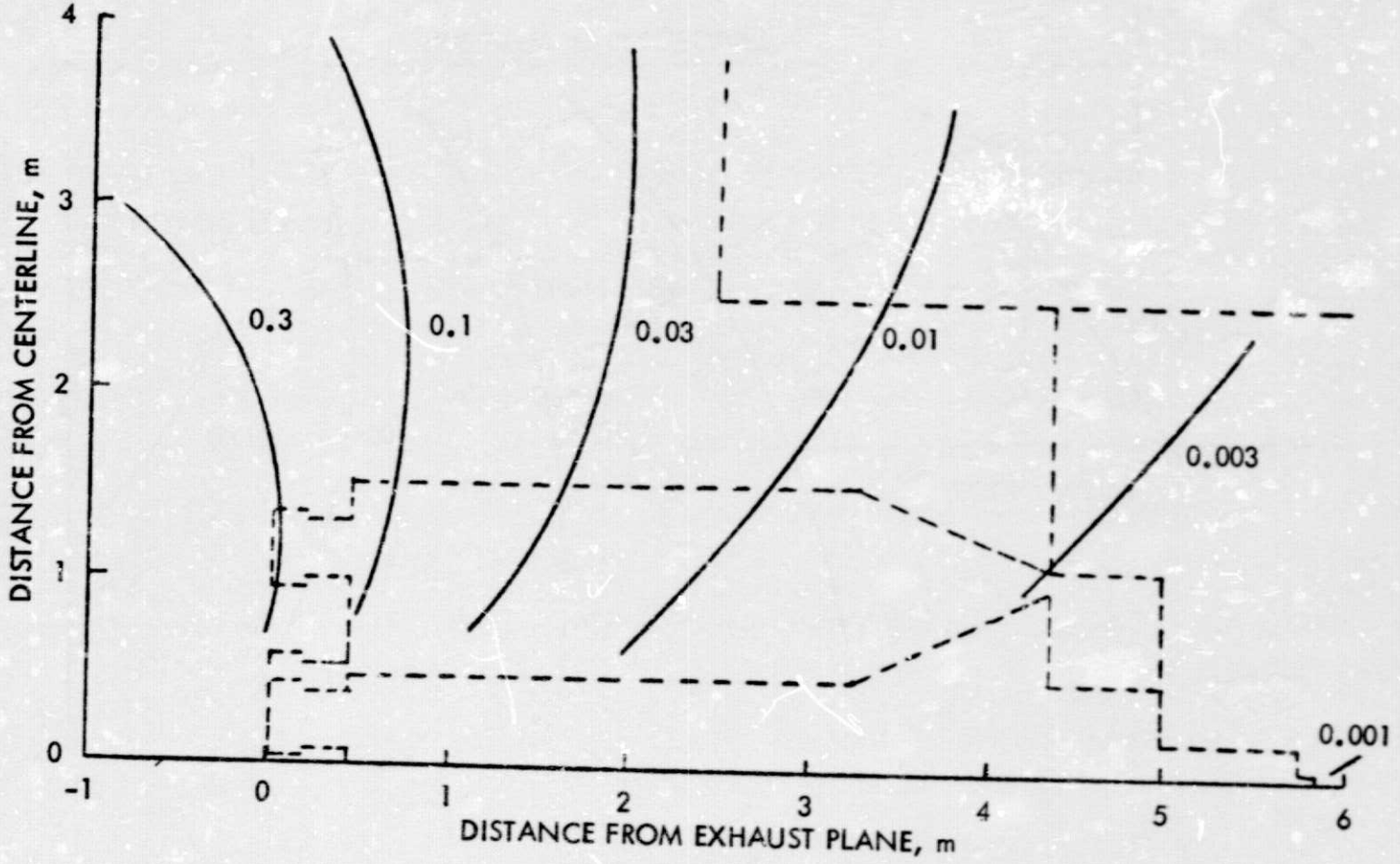

Figure 5. Saturation Electron Current Density, A/m^2, for Assumed Spacecraft Configuration

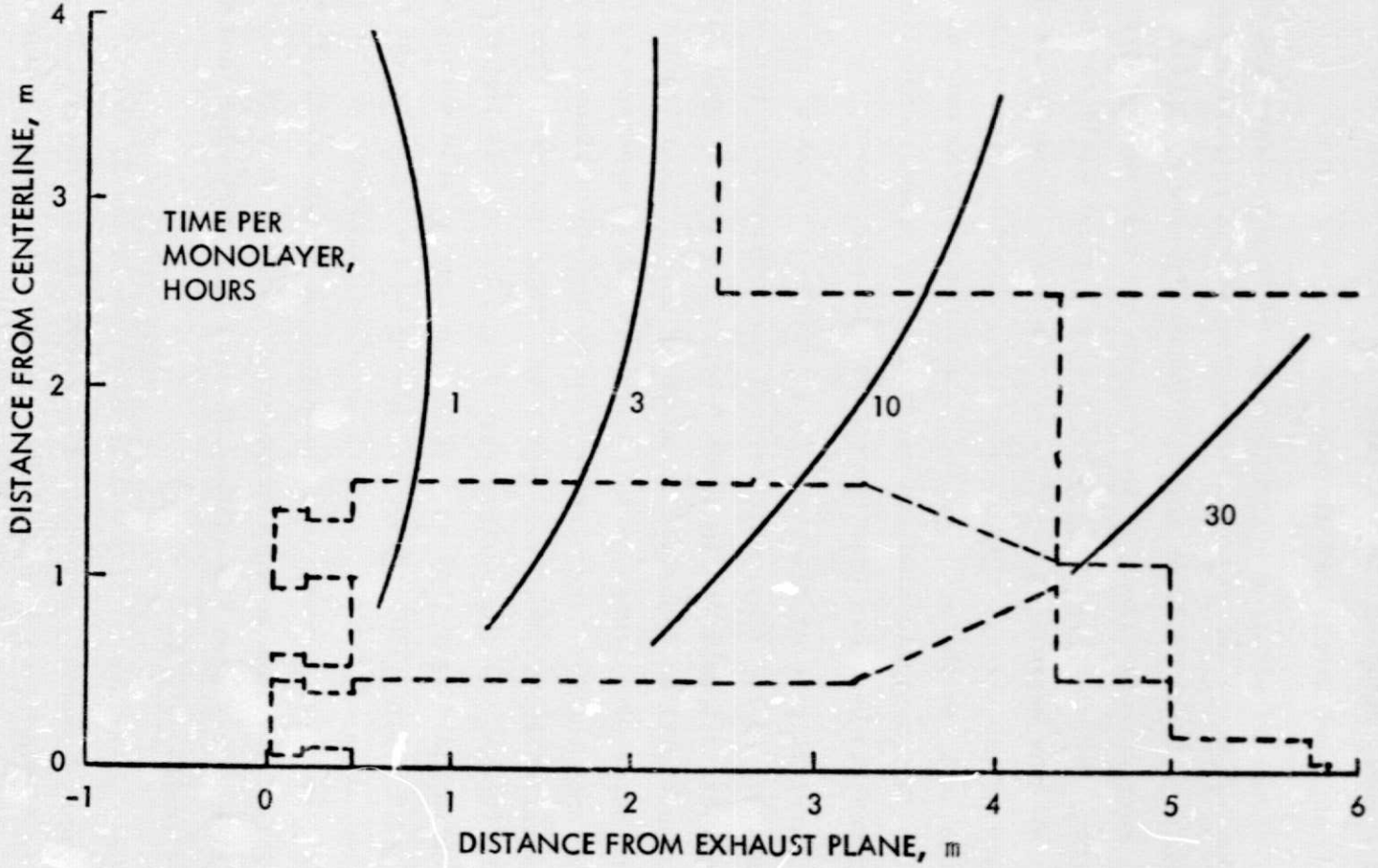

Figure 6. Arrival Rate of Hg^+, Expressed as Time for Monolayer (Sticking Depends on Surface Conditions)

and most of the electrons will be reflected. Negative surfaces will reflect electrons and collect only ions, but this effect appears to be of little value in significantly reducing the upstream flow of the charge-exchange plasma.

2. Discussion of Sample Calculation

The amount of electron current collected by a positive and exposed solar-cell array is one of the significant results of the calculation presented above. A high voltage array would be more seriously affected by a fixed level of electron current collection, so the results are also voltage dependent. For a 400 V array, for example, the 1.7 A electron current would correspond to a maximum loss of ∿680 watts. If there is a significant variation in voltage along the length of the array, this loss can be reduced by placing the high voltage end of the array at the outboard end, where the electron current density is smallest. This approximation assumes there are exposed conducting paths for the electrons to be drawn from the charge-exchange plasma.

The arrival rate of electrons is a maximum of 14 mA/m^2 on the solar array (see Fig. 3). By Eq. (3a), this arrival rate corresponds to a monolayer buildup of mercury at that position in about 6 hours. A 1000 Å layer with near zero transmittance will be deposited in about 83 days. Significant effects are likely to occur with layers less than 1000 Å. From experience with mercury vapor, we know that no accumulation occurs when the surface involved is above the evaporation temperature for that rate. There are still two reasons to be concerned though. If the surface should fall below this temperature, an accumulation will occur that will require a considerable excess of temperature to evaporate again. This could very likely be the case for the exterior of the sun-shaded sides of thermal blankets, passive radiators, and other spacecraft surfaces. Once the mercury is accumulated, it may be difficult to evaporate away. This is because mercury evaporation can be orders of magnitude below equilibrium values when the surface is less than very clean and the temperature is below roughly 100°C.

A less clear aspect of possible Hg accumulation is that the arriving Hg is ionized and is probably arriving with several eV of energy. Because 1 eV corresponds to 11,600°K, we should not be too hasty in assuming that no damage will occur.

3. Limitations of Model Accuracy

Most of the limitations associated with the Hg charge-exchange model and calculation have been mentioned earlier. They will be summarized here for completeness.

The model was obtained from tests of rather simple configurations, hence is not suited to estimating the effects of nonsymmetrical thruster arrays and complicated spacecraft shapes. Even the effects of surface orientation are not fully understood.

The electron temperature in the charge-exchange plasma is an important, but only partially evaluated parameter. We know that smaller thrusters tend to have higher temperatures in this plasma, but we do not know if arrays of thrusters will depart from the values obtained with single thrusters. We also know that initial neutral velocity will be more important at small electron temperatures, resulting in a bias of charge-exchange ion trajectories in the downstream direction. The magnitude of this bias, though, has not been evaluated.

Finally, there is an electron temperature effect that has not been mentioned. The space environment includes a plasma. The electrons of this space plasma will interact with the electrons of the charge-exchange plasma, possibly resulting in a different electron temperature than obtained in ground tests. This effect will be discussed in the section, Electron Temperature in Space.

The uncertainties that now exist in the model are summarized in Fig. 7.

C. MOLYBDENUM CHARGE-EXCHANGE MODEL

As mentioned in the introduction, a small fraction of the Mo atoms that are sputtered from the accelerator grid charge exchange with beam Hg ions downstream of the thruster. These Mo charge-exchange ions share the ability of Hg charge-exchange ions to flow around obstacles. As will be shown, the rate of production of Mo ions is very low compared to that of Hg ions. It is therefore difficult to make an experimental evaluation of Mo ions. At this time, only a simple theoretical analysis can be presented, based on the Hg charge-exchange model presented previously.

Thrusters		Simulated Spacecraft	Test Location	T_c,CV	Uncertainty Factor		
No.	Size				T_e	η_e	j_e
1	5-15 cm		Ground	2.5-3.5	2X	2X	2X
1	30 cm		Ground	0.1-0.2	2X	∿4X	∿2X
7	30 cm	Simple	Ground	0.1-0.2	∿2X	∿8X	∿4X
7	30 cm	Simple	Space	0.1-20*	∿4X	∿10X	∿6X
7	30 cm	Complex	Space	0.1-20*	Larger than above		

*Dependent on charge-exchange and space plasmas' densities and temperatures

Figure 7. Estimates of Uncertainties

The approach used is to compare the production rates of Hg and Mo charge-exchange ions. The Mo ions are assumed to be distributed in the same manner as the Hg ions, but lower by a factor corresponding to the lower production rate. This approach ignores the much higher initial velocities of the Mo neutrals. These higher velocities will result in a bias of trajectories in the downstream direction. The arrival rates of Mo ions in the upstream hemisphere should, due to this effect, be less than calculated.

The production rate of Hg charge-exchange ions is

$$\dot{N}_{ce} = \frac{2J_b^2(1 - \eta_u)\sigma}{\pi r_b \eta_u q^2 \bar{v}_o} , \tag{4}$$

where q is the electronic charge, $\bar{v}_o$ is the average neutral velocity before charge exchange, σ is the charge-exchange cross section, and the other parameters are the same as defined earlier. A similar production rate for Mo charge exchange ions is

$$\dot{N}_{ce,Mo} = \frac{2F_a J_b^2 Y\sigma}{\pi r_b q^2 \bar{v}_o} , \tag{5}$$

where, in addition to previously defined variables, F_a is the ratio of accelerator impingement current to beam current, and Y is the sputter yield in atoms/ion.

The ratio of Mo to Hg charge-exchange rates is obtained by dividing Eq. (5) by Eq. (4). With the use of Hg and Mo subscripts where appropriate, this ratio is

$$\frac{\dot{N}_{ce,Mo}}{\dot{N}_{ce,Hg}} = \frac{F_a Y \eta_u \sigma_{Mo} \bar{v}_{o,Hg}}{(1 - \eta_u)\, \sigma_{Hg} \bar{v}_{o,Mo}} . \tag{6}$$

For the 30-cm thruster, the value of F_a is about 0.0025,[12] the value of Y for 1000 eV Hg ions is approximately 1.0,[13] $\sigma_{Mo}(Hg^+ + Mo \rightarrow Hg + Mo^+)$ is about 1×10^{-19} m^2,[14] $\sigma_{Hg}(Hg^+ + Hg \rightarrow Hg + Hg^+)$ is about 6×10^{-19} m^2,[15-17] $\bar{v}_{o,Mo}$ is

about 7×10^3 m/sec,[18] $v_{o,Hg}$ is about 230 m/sec (500°K), and η_u is again 0.9. With these substitutions, Eq. (6) becomes

$$\dot{N}_{ce,Mo}/\dot{N}_{ce,Hg} = 1.2 \times 10^{-4} \tag{7}$$

The uncertainty in this calculation is due to the uncertainty of distribution and yield of sputtered Mo for an operating thruster, the uncertainty of mean neutral velocity (the datum used here was for Kr^+ on Mo), the uncertainty in bombarding ion energy, and the additional bias on Mo ion trajectories due to the initial high neutral energies. All of these additional uncertainties beyond those of charge-exchange Hg are estimated to raise the factor of uncertainty from four for Hg ions to ten for Mo ions.

Equations (3) and (7), together with the electronic charge, can be used to translate the electron current density of Fig. (5) to Mo ion arrival rate per unit area. The ratio is

$$\dot{N}_{Mo}/A = 4.4 \times 10^{12}\ j_e,\ N_{Mo} \cdot m^{-2} - sec^{-1} \tag{8}$$

This ratio was used to obtain Fig. 8.

A monolayer (2.5 Å) of Mo atoms is about $1.6 \times 10^{19}/m^2$ (as compared to about $1.2 \times 10^{19}/m^2$ (2.9 Å) for Hg). For the region of the solar array with the maximum of 14 mA/m^2 of electron current, then, a monolayer would be expected to take 72,000 hours. Even with a factor of 10 increase in rate due to the estimated inaccuracy of the calculations, it would take over a year for a monolayer to form.

In situ measurements of transmittance have been made using films of the sputtered efflux from thrusters (mostly Mo).[5] These films were primarily from deposition of neutrals, rather than the charge-exchange Mo ions considered in this section. These results, however, should give an indication of the deposition effects to be expected. The total transmittance was not linear with time. It ranged from about 0.75 at 30 Å thickness, to about 0.50 at 100 Å, to about 0 at 1000 Å. It appears, though, that assuming a linear variation is conservative below 30 Å thickness. A monolayer of Mo should give about a 2.5 percent reduction in transmittance.

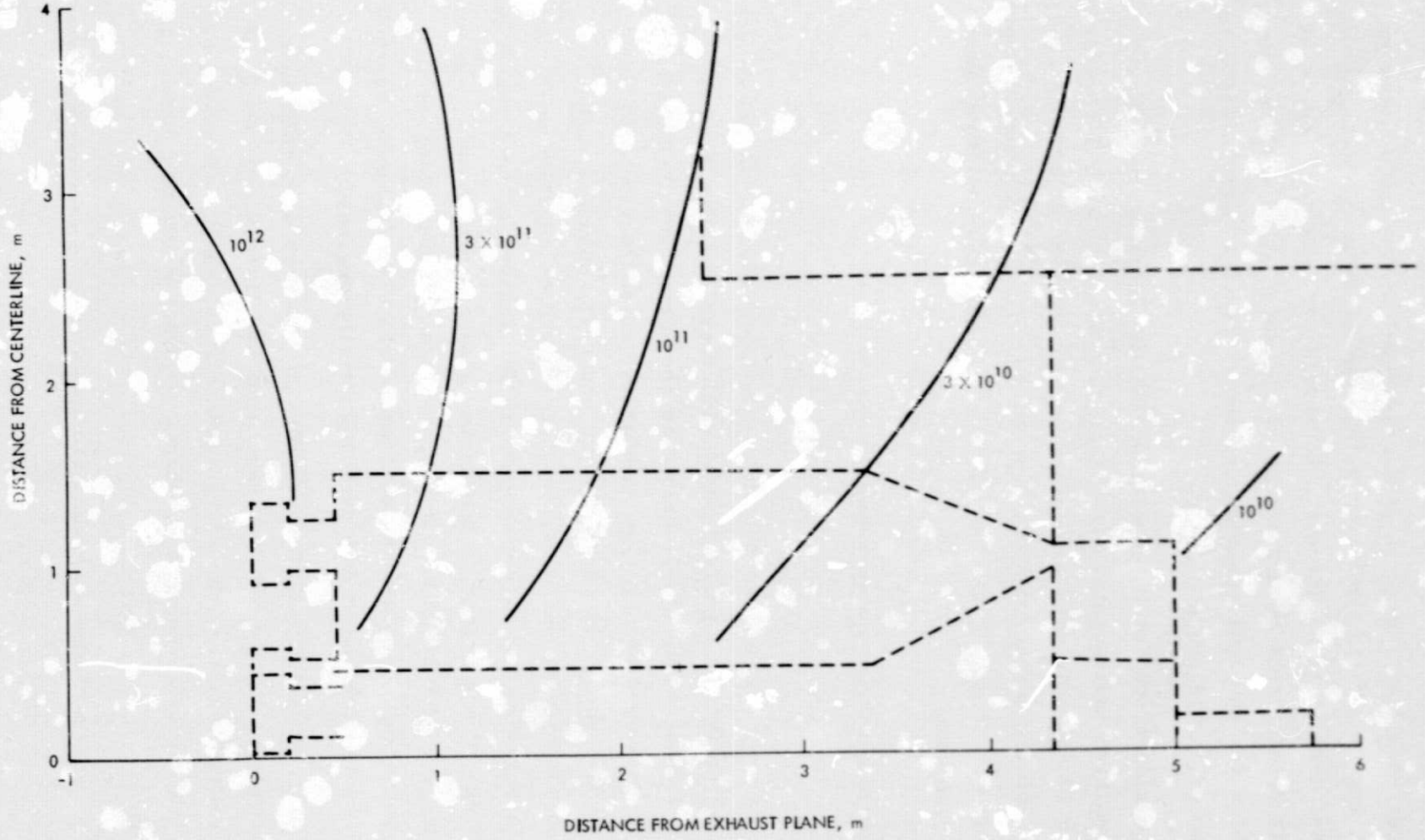

Figure 8. M_o^+ Arrival Rate, No/m^2-sec

For the worst case (ten times the predicted rate) at the worst location on the solar array, over 1 year of operation with 7 thrusters would be required to give a 2.5 percent loss in transmittance. Because other locations should be less affected, it appears that Mo deposition on the solar array will not be a significant problem for the configuration studied. A much closer location to the thruster, though, could cause problems.

The major consideration for Mo deposition (in the upstream hemisphere) appears to be sensitive instruments, optical or otherwise, that will be adversely affected by 10 to 100 percent of a monolayer. A monolayer on solar cell surfaces with a normal emissivity (ε) of 0.85 will produce $\varepsilon \sim 0.7$.[19] Molybdenum deposition could have an effect on thermal surfaces such as passive radiators used to cool instrument components.

D. CHARGE-EXCHANGE MEASUREMENTS IN GROUND TESTS

1. Mercury

The Hg ions make up the bulk of the charge-exchange plasma. Measurements of this plasma density (with Langmuir probes) will therefore give a close indication of the density of Hg ions. As described in the experimental studies,[8-10] the ions should be collected by negative boundaries, so reflection will not be a limitation on measurements. In fact, plasmas generally assume a potential more positive than surrounding surfaces, so that the proper negative wall bias is automatically attained. The only exception is for regions of very low density so that the total electron currents to boundaries associated with such regions is still quite small. Under these conditions the local plasma potential will be governed by wall potential. A moderate additional wall bias (relative to the beam target) will avoid problems in the very low density regions.

Some additional calculations or measurements are desirable to make sure that most of the charge-exchange ions are generated immediately downstream of the thruster(s), rather than from the background neutral density all along the beam(s). To meet this latter requirement simply requires a low enough facility background pressure.

The measurement of Hg charge-exchange effects is thus readily accomplished in ground tests.

2. Molybdenum

The measurement of Mo charge exchange ions poses much more difficult problems. One major problem is the background level of sputtered Mo atoms. To show the magnitude of this problem, it is necessary to go through a simple analysis.

The loss rate of sputtered Mo atoms from the accelerator grid is

$$\dot{1}_o = F_a J_b Y/q \qquad (9)$$

where all the parameters are defined the same as previously. This rate is probably an upper limit for Mo atoms in the downstream direction in that not all accelerator grid impingement is on the downstream side.

Assuming a frozen Hg target in the ground facility to minimize contamination with other sputtered material, the arrival rate of Mo atoms at this target is due to an approximately cosine distribution from the accelerator grid. Sputter pits will develop (midway between each group of three adjacent holes) on the downstream side of the accelerator grid. As this occurs, the distribution will depart from a cosine, but the departure will primarily be restricted to large angles from the beam direction. The rate of Mo arriving at the target should be nearly unchanged by these pits. The cosine distribution corresponds to a uniform arrival rate at the sphere shown in Fig. 9. The effective diameter of the beam at the target is d_t, with a corresponding area of A_t. This diameter is best determined experimentally, using the diameter over which the frozen Hg experiences net sputtering. Outside of this diameter the sputtered Mo will tend to be trapped within the condensing Hg vapor. From geometrical considerations, (Fig. 9), the fraction of sputtered Mo atoms that will be resputtered from the target is approximately the solid angle $A_t/(\ell_t/2)^2$ divided by the total sphere solid angle of 4π. The resputtered fraction is thus

$$F_{rs} = A_t/\pi\ell_t^2. \qquad (10)$$

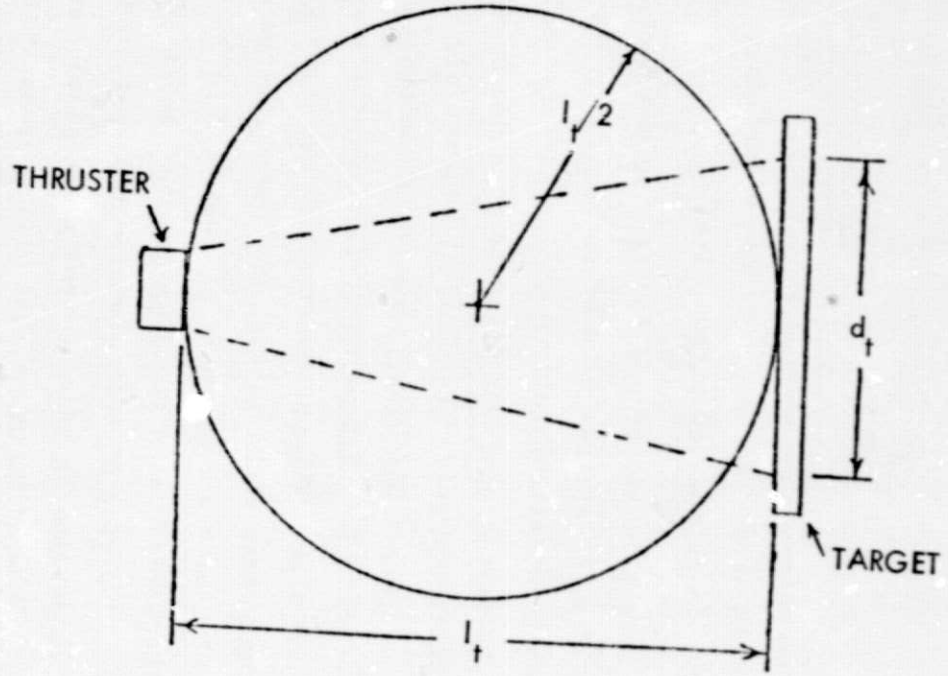

Figure 9. Thruster and Frozen Mercury Target in Ground Facility

A similar fraction can be determined for the fraction of resputtered Mo atoms that arrive at a sample coupon. Assuming that this coupon is in the plane of the accelerator system and at a radius R from the thruster, with $R<<\ell_t$,

$$F_c = A_c/\pi\ell_t^2 \quad . \tag{11}$$

Multiplying Eqs. (9) through (11) to obtain the arrival rate of neutral atoms at the coupon area A_c,

$$\dot{N}_{o,c} = F_a J_b Y A_c A_t/\pi^2 q \ell_t^4 \quad . \tag{12}$$

This rate can be compared to the arrival rate of charge-exchange Mo ions at the same location, using the preceding Mo model. From Eqs. (2), (3), and (6), together with the Table II parameter for 90 deg.,

$$\dot{N}_{ce,c} = 7.1 \times 10^{-4} A_c F_a J_n^2 Y \sigma_{Mo} \bar{v}_{o,Hg}/q r_b R^2 \sigma_{i,g} \bar{v}_{o,Mo} \quad . \tag{13}$$

The neutral Mo to charge-exchange Mo arrival rate ratio is Eq. (12) divided by Eq. (13),

$$\dot{N}_{o,c}/\dot{N}_{ce,c} = 140\ A_t r_b R^2 \sigma_{Hg} \bar{v}_{o,Mo}/\ell_t^4 J_b \sigma_{Mo} \bar{v}_{o,Hg} \quad . \tag{14}$$

Assume a 30-cm thruster, so that J_b is 2A and r_b is 0.14 m. For the other values we will assume 3.5 m for ℓ_t, 3.6 m^2 for A_t (±15 deg.), 0.5 m for R, and previously used values for q, σ_{Hg}, σ_{Mo}, $\bar{v}_{o,Hg}$, and $\bar{v}_{o,Mo}$. With these substitutions, Eq. (14) becomes

$$\dot{N}_{o,c}/\dot{N}_{ce,c} = 21. \tag{15}$$

The Mo neutrals come from the target from the general downstream direction, while the Mo charge-exchange ions are generally moving radially outwards, so some separation can be made by using the proper angle and shielding for the coupon area, A_c. With a "noise" level 21 times the "signal" level, though, it may be still difficult to separate out the Mo charge-exchange rate by deposition. Also, although resputtered Mo atoms will have a "sticking" coefficient near unity, it will still be less than unity. A small percentage of Mo atoms reflected from the walls of the vacuum facility will add a nearly isotropic component that will be hard to shield.

Detection of Mo ions is a possible alternative, but this will require momentum analysis to discriminate from the nearly 10^4 times higher background of Hg charge-exchange ions (Eq. (7)). Also the rate of Mo ions is small in absolute terms. For the location used above for comparison of neutral and charged Mo, the current of Mo ions through 1 cm^2 aperture (which is large for most momentum analysis) is only 10^{-10} A.

In summary, then, experimental detection of Mo charge-exchange ions is difficult in a ground test.

E. ELECTRON TEMPERATURE IN SPACE

The charge-exchange plasma in a ground facility fills, with varying degrees of density, the entire facility volume. The electrons in this plasma have long mean free paths, so that with sufficient energy they can pass through any part of the available volume. The electrons in both the beam and the charge-exchange plasma travel much faster than the ions. Current neutrality will therefore require, on the average, a number of electrons to be reflected at the boundaries for each one that escapes.

In space, the charge-exchange plasma must eventually blend into the ambient space plasma, rather than be terminated abruptly at facility walls. A preliminary model of the interactions or ion drive propulsion with this space plasma is presented in this section.

1. Space Plasma

Two regions in space are considered for this interaction with the ambient plasma. One is a low earth orbit, where an ion drive vehicle might be expected to start an orbit raising operation. The other is interplanetary space at the radius of earth's orbit from the sun. These two regions are by no means a complete inventory of ion drive environment. They are, however, sufficient to show the major problems involved.

The low earth orbit ($\sim$150 nautical miles) has low energy electrons (0.1 - 0.2 eV) at a high density ($\sim 10^6$ cm^{-3}).[20] For interplanetary space, the electron energy is much higher (10 - 20 eV) and the density much lower (5 - 20 cm^{-3}).[21,22]

2. Distance of Interaction

The solar wind in interplanetary space travels radially outward from the sun and the magnetic field lines are frozen into this plasma.[21] The magnetic Reynolds number can be used to assess the interaction of this magnetic field with the charge-exchange plasma. The magnetic Reynolds number is given by,[23]

$$R_m = \mu \sigma v \ell ,$$

where σ is plasma conductivity, and v and ℓ are the typical velocity and length, respectively, of the situation in question. Taking the permeability, $\mu = \mu_o$, and for reasonable values of σ, v, and ℓ for the magnetic field moving into the charge-exchange plasma, $R_m \gg 1$. For this case penetration of the magnetic field is very slow and the full pressure gradient, $B^2/2\mu_o$, can develop.[23] Assuming a simple interface, the relation

$$n_i m_i v^2 = \frac{B^2}{2\mu_o} \tag{16}$$

will give an estimate of where the magnetic field gradient exists. In the frame of stationary B, the charge-exchange plasma velocity, v, will roughly be that of the solar wind. Solving Eq. (16) for n_i, ion density, and using Eq. (1), R is found to be equal $\sim 10^2$ km, where m_i is the charge-exchange ion's mass. Because the magnetic field strength is $\sim 2 \times 10^{-5}$ gauss at 1 AU, the Larmor radius is $\sim 10^3$ km. The magnetic field will decrease as the radial distance from the sun increases and the Larmor radius likewise will increase. This is a very simple

picture for a complex problem. However, it points out that for most situations the space plasma will exist around the spacecraft and not be affected by the solar wind's magnetic field.

A rough measure of the transition distance between the charge-exchange plasma and the space plasma is where their densities are equal. The procedure for calculating the Hg charge-exchange plasma has been described and has been used for calculating the equal-density radius at 90 and 180 deg. to the beam direction. This equal-density radius may also be of interest for the ion beam. For the latter calculation, the ion beam current was assumed confined to a ±15 deg. exhaust cone. The results of these calculations are shown in Table III.

The distance 180 deg. to beam direction for Low Orbit is readily available in a ground facility. The distance 90 deg. to beam direction for low orbit is available only at the very largest facilities. All other distances exceed the dimensions of the largest ground facilities. It therefore does not appear possible to simulate this interaction in a ground facility.

3. Electron Interactions

As indicated above, the electrons are much more mobile than ions, so that in a ground vacuum facility there will be many electron collisions with the facility boundaries for each electron that escapes. In space, there are two alternatives. A potential well can be formed by the plasma near the spacecraft, so that electrons are reflected at the boundaries of this well, similar to the reflection at the boundaries of a ground facility. Or the electrons in the charge-exchange plasma can escape, and be replaced by ambient space electrons.

Table III. Equal Density Radii

Direction Relative to Ion Beam	Low Orbit (10^6 cm^{-3})	Interplanetary (10 cm^{-3})
0 deg.	120. m	40 km
90 deg.	16. m	5 km
180 deg.	2. m	0.5 km

To show the magnitude of the problem, the electron escape rates were calculated for the case where no reflection occurred. For the ion beam, the electron escape rate was 46 A. For the entire charge-exchange plasma it was 24 A. With a total electron escape rate of 70 A, and only a 14 A ion escape rate in the beam, 56 A of electrons would need to be either reflected or collected from space to maintain spacecraft and plasma neutrality. The rate of electron exchange with space can clearly be quite large. Whether or not this exchange takes place will depend on collision processes for the electrons.

For interplanetary space, the interaction volume is quite large (Table III). To simplify the calculations, we will assume a sphere with a radius of 5 km for the charge-exchange plasma volume. Integrating the total number of charge-exchange electron/ion pairs in this volume gives about 1.1×10^{19}. At 3000 sec., the ion beam adds another 1.5×10^{19} electron/ion pairs in this volume. This gives a total of about 2.6×10^{19} electron/ion pairs within 5 km of the spacecraft. In comparison, the total number of Hg neutrals within this sphere is 2.1×10^{20}. In the 10 - 20 eV electron energy range, the excitation/ionization cross section of Hg is several times 10^{-20} m^2, while the Coulomb collision cross section of electrons is of the order of 10^{-18} m^2. Clearly, then, Coulomb collisions of space electrons with electrons near the spacecraft will be the dominant mechanism for capture of these high velocity, but less dense, space electrons. (Coulomb collisions with ions or elastic collisions with neutrals are not significant because of the small energy transferred.)

At 15 eV, the space electrons have an average velocity of 2.6×10^6 m/sec. For a 10^7 m^{-3} density, the space electrons should have a collision frequency of

$$\nu = n\bar{v}\sigma = 10^7 \times 2.6 \times 10^6 \times 10^{-18} = 2.6 \times 10^{-5} \qquad (17)$$

with each low energy electron in the 5 km radius sphere. For the entire 2.6×10^{19} electrons, this would give a capture rate of

$$\dot{N}_{capt} = 2.6 \times 10^{19} \times 2.6 \times 10^{-5} = 6.8 \times 10^{14} . \qquad (18)$$

Multiplying this rate by the electronic charge, q, gives a capture current of about 100 μA.

Comparing this electron capture rate with the possible net loss of 56 A clearly shows that capture of ambient space electrons will not be a significant process in interplanetary space. It seems reasonable to conclude, then, that the two electron populations will coexist in space with negligible interaction, similar to the two-group theory of electrons in a thruster discharge chamber. The low energy electrons must therefore be reflected to maintain charge neutrality with ions. The reflection would be expected near the surface where spacecraft plasma density equals ambient space plasma density.

At low orbit ambient conditions, the situation is considerably different. The ambient electron temperature is roughly the same as that of the charge-exchange plasma. There should therefore be no significant distinction between an escaping charge-exchange electron and a captured ambient space electron. The plasma surrounding the spacecraft should thus blend smoothly with the ambient plasma.

There is another case that is worth considering. A smaller thruster, such as might be used for spacecraft attitude control, stationkeeping, or drag makeup, would be expected to have a higher electron temperature. With a higher than ambient temperature, the space electrons would be captured while the higher energy electrons from the spacecraft would escape. One would therefore expect the electron temperature near a spacecraft to be governed by the ambient space value when that value is less than the value obtained in a ground test.

As had been mentioned earlier, the ion (and therefore electron) density is related to the Bohm, or ion acoustic velocity. We should address quantitatively the question of the effect the ambient plasma may have on this velocity. Two plasmas of different density and electron temperature will be occupying the same space. What electron temperature will govern the ion velocity? The Bohm velocity,

$$v_B = \sqrt{KT_e/m_i} \quad , \tag{19}$$

can be thought of as the velocity an ion will have after being accelerated through a potential, V_o. Therefore,

$$v_B = \sqrt{\frac{2q\,|V_o|}{m_i}} \tag{20}$$

For the case of a plasma with two Maxwellian electron velocity distributions having different electron temperatures and densities, the following relation can be obtained:[24]

$$V_o = \frac{k}{2q} \frac{\left\{ n_1 \exp\left(\frac{qV_o}{kT_1}\right) + n_2 \exp\left(\frac{qV_o}{kT_2}\right) \right\} T_1 T_2}{n_1 T_2 \exp\left(\frac{qV_o}{kT_1}\right) + n_2 T_1 \exp\left(\frac{qV_o}{kT_2}\right)} \tag{21}$$

For typical densities and temperatures of the primary beam plasma and the interplanetary space plasma, the beam plasma is by far the dominating factor in establishing the Bohm velocity.

For typical values of the solar wind at 1 AU and the charge-exchange plasma from a single thruster, the dynamic pressure, $m_i n_i v_i^2$, of the solar wind and charge-exchange plasma are roughly equivalent a few tens of meters from the spacecraft. This distance will increase as the spacecraft's distance from the sun increases, and as the number of thrusters operating increases. Because one pressure does not overwhelm the other, each individual case of position relative to the sun, number of operating thrusters, and solar wind activity will have to be calculated to determine this boundary. However, since the mean free path for the situations discussed is in the multiple kilometers range, the flow of the charge-exchange plasma around the spacecraft should not be affected by the solar wind ions.

4. Discussion

The proposed interactions with the space plasma appear reasonable. Ground verification, however, ranges from difficult to effectively impossible. Plasma calculations have frequently been found invalid in the past. The reason for

the lack of validity has often been collective interactions, which can be very difficult to predict. No collective interactions were considered in this analysis.

F. CONCLUDING REMARKS

The Hg charge-exchange model described appears adequate for preliminary estimates of solar array and spacecraft interactions. The electron densities predicted by this model are subject to electron temperature uncertainties due to the variation that might be expected with thruster size, the clustering of thrusters and the interaction with the space plasma. There are other effects that introduce uncertainty in both electron density and saturation electron current density. They are the relative electron and neutral temperatures (which result in more or less trajectory bias for the charge exchange ions in the downstream direction) and the departure from axial symmetry for the thruster array. All of these effects are estimated to introduce a factor of several uncertainty in the calculations. In addition, the model is not capable of predicting detailed spacecraft shape and surface orientation effects on charge-exchange ion trajectories.

The Hg charge-exchange model, though, is adequate for predicting the rough magnitude of the electron collection problem at the solar array. It can also be used to estimate the plasma environments for spacecraft science instruments. The arrival rate of Hg ions and possible condensation problems can also be evaluated.

The possibility of surface reactions due to colliding Hg charge-exchange ions remains an unknown. Experience with Hg vapor indicates no problem should be expected. Experience with several eV Hg ions, though, is much more limited. The rate of Hg ion arrival is high enough for much of the spacecraft that coverage could become a serious problem if ions cause reactions on some surfaces that inhibit subsequent vaporization.

The Mo charge-exchange model has a larger uncertainty than the Hg model. It appears, however, that there will be no major problems with Mo deposition. The amount of deposition could still be a problem for certain sensitive instruments and thermal surfaces near the thrusters. Reducing the uncertainty in Mo deposition appears difficult with ground tests.

To summarize, there appear to be no major obstacles to the use of ion drive. There are areas where spacecraft/ion drive interactions exist, but can be controlled through the use of proper design approaches. There are also areas where uncertainties exist that could cause later problems with sensitive instruments or surfaces. Resolution of these uncertainties is recommended early in the ion drive program to avoid the possible greater expense and schedule impact of delayed resolution.

G. REFERENCES

1. J. F. Staggs, W. P. Gula, and W. R. Kerslake, "Distribution of Neutral Atoms and Charge-Exchange Ions Downstream of an Ion Thruster", J. Space. Rock., Vol. 5, pp. 159-164, Feb. 1968.

2. T. W. Reynolds and E. A. Richley, "Contamination of Spacecraft Surface Downstream of a Kaufman Thruster", NASA Tech. Note TN D-7038, Jan. 1971.

3. T. W. Reynolds, "Procedure for Estimating Effects of Ion Beam Interaction with Spacecraft", NASA Tech. Memo. TM X-68043, Apr. 1972.

4. J. V. Staskus and R. J. Burns, "Deposition of Ion Thruster Effluents on SERI II Spacecraft Surfaces", AIAA Paper No. 70-1128, Aug. 1970.

5. A. J. Weigand and M. J. Mirtich, "Measurement of Sputtered Efflux from 5-, 8-, and 30-cm Diameter Mercury Ion Thrusters", AIAA Paper No. 75-358, Mar. 1975.

6. W. R. Kerslake, "Charge-Exchange Effects on the Accelerator Impingement of an Electron-Bombardment Ion Rocket", NASA Tech. Note TN D-1657, May 1963.

7. J. V. Dugan, Jr., "Upper-Limit Charge Exchange Cross Sections for Mercury$^+$ on Molybdenum and Cesium$^+$ on Aluminum", NASA Tech. Memo. TM X-2427, Mar. 1972.

8. H. R. Kaufman, "Charge-Exchange Plasma Generated by an Ion Thruster", NASA Contr. Rep. CR-134844, June 1975.

9. H. R. Kaufman, "Interaction of a Solar Array with an Ion Thruster Due to the Charge-Exchange Plasma", NASA Contr. Rep. CR-135099, Oct. 1976.

10. H. R. Kaufman, "Charge-Exchange Plasma Generated by an Ion Thruster", NASA Contr. Rep. CR-135318, Dec. 1977.

11. G. K. Komatsu, R. K. Cole, D. K. Hoffmaster, and J. M. Sellen, Jr., AIAA Paper No. 75-428.

12. C. Collett et al. "Fabrication and Qualification Testing of ETM 30 cm Diameter Ion Thrusters", NASA Contr. Rep. CR-135193, Apr. 1977.

13. K. Meyer and A. Guntherschulze, "Kathodenzerstaubung in Quecksilberdampf bei sehr geringen Drucken", Z. Physik, Vol. 71, pp. 277-290 (1931).

14. D. A. Vroom and J. A. Rutherford, "Cross Sections for Charge Transfer between Mercury Ions and other Metals", NASA Contr. Rep. CR-135205, June 1977.

15. R. M. Kushnir, B. M. Palyukh, and L. A. Sena, "Investigation of Resonance Charge Exchange in Monatomic Gases and Metal Vapors", Bull. Acad. Sci. USSR - Phys. Ser., Vol. 23, pp. 995-999, Aug. 1959.

16. I.P. Iovitsu and N. Ionescu-Pallas, "Resonant Charge-Exchange and the Kinetics of Ions", Soviet Physics Tech. Physics, Vol. 4, pp. 781-791, 1960.

17. D. Zuccaro, "Measurement of the Charge Exchange Cross Section of Mercury", NASA Contr. Rep. CR-72398, Apr. 1968.

18. G. K. Wehner and G. S. Anderson, "The Nature of Physical Sputtering", Chap. 3 in Handbook of Thin Film Technology (L. I. Maissel and R. Glang, eds.), McGraw-Hill Book Company, New York, 1970.

19. D. F. Hall, "Electrostatic Propulsion Beam Divergence Effects on Spacecraft Surfaces", Vol. II, Jan. 1973.

20. U. Samir, "Spacecraft/Spaceplasma Interaction", Spaceflight, Vol. 10, No. 8, August, 1968.

21. E. N. Parker, Interplanetary Dynamical Processes, Wiley and Sons, New York, 1963.

22. T. N. Divine, "Interplanetary Charged Particle Environments", JPL-TM-33-637, August, 1973.

23. H. K. Messerle, "Other Plasma Phenomena and Possible Applications", Discharge and Plasma Physics, (S.C. Haydon, ed.), The University of New England, 1964.

24. K. Uehara, et al., "Ion Saturation Current of a Plasma Having Two Electron Temperatures", Japanese Journal of Applied Physics, Vol. 14, No. 11, pp. 1761-1764, Nov. 1975.

NASA—JPL—Coml., L.A., Calif.